ELSEVIER

Engineered spider silk-based 2D and 3D materials prevent microbial infestation

Sushma Kumari [1,†], Gregor Lang [1,2,†], Elise DeSimone [1], Christian Spengler [3], Vanessa T. Trossmann [1], Susanne Lücker [4], Martina Hudel [5], Karin Jacobs [3], Norbert Krämer [4], Thomas Scheibel [1,6,7,8,9,*]

[1] Department of Biomaterials, Faculty of Engineering Science, University of Bayreuth, Prof.-Rüdiger-Bormann-Str. 1, 95447 Bayreuth, Germany
[2] Biopolymer Processing Group, Faculty of Engineering Science, University of Bayreuth, Ludwig-Thoma-Str. 36A, 95447 Bayreuth, Germany
[3] Department of Experimental Physics and Center for Biophysics, Saarland University, 66123 Saarbrücken, Germany
[4] Medical Center for Dentistry, Department of Paediatric Dentistry, Medical Center Gießen and Marburg, Justus-Liebig University Gießen, Schlagenzahl 14, 35392 Gießen, Germany
[5] Institute of Medical Microbiology, Justus-Liebig University Gießen, Schubertstraße 81, 35392 Gießen, Germany
[6] Bayreuth Center for Material Science and Engineering (BayMAT), Germany
[7] Bavarian Polymer Institute (BPI), Germany
[8] Bayreuth Center for Colloids and Interfaces (BZKG), Germany
[9] Bayreuth Center for Molecular Biosciences (BZMB), University of Bayreuth, Universitätsstraße 30, 95447 Bayreuth, Germany

Biofilm formation, especially of antimicrobiotic-resistant microbial strains, are a major problem in health care. Therefore, there is great interest in developing advanced materials that are selectively inhibiting microbial adhesion to surfaces, but at the same time promoting mammalian cell growth. In nature, some spider silks have evolved to repel microbes, a feature that could be used in biomaterials. To unravel how microbe repellence can be achieved in engineered spider silk, different recombinant spider silk proteins based on the consensus sequences of *Araneus diadematus* dragline silk proteins (fibroin 3 and 4) were processed into 2D-patterned films and 3D-hydrogels. Strikingly, protein structure characteristics on the nanoscale are the basis for the detected microbe-repellence. Designed spider silk materials promoted mammalian cell attachment and proliferation while inhibiting microbial infestation, demonstrating the great potential of these engineered spider silk-based materials as bio-selective microbial-resistant coatings in biomedical as well as technical applications.

Introduction

Pathogenic microbial contaminations of surfaces, when exposed to patients, significantly increase the risk of infection, and represent a severe problem in the public health care sector [1,2]. Biofilm formation on biomedical devices, such as prosthetics, medical implants, contact lenses, and catheters, not only limits their functionality and lifetime but can also cause life-threatening infections [3,4]. Consequently, microbial biofilm generation and nosocomial infection during conventional medical therapy have significantly increased mortality as well as healthcare costs worldwide in the last decade. Outside of the clinical setting, diseases associated with food contamination as well as biofouling of material surfaces in contact with water supply systems are considered major health issues [5]. There are several interacting parameters that have ultimately led to this problem, however, the most critical is the evolution of antimicrobial-resistant (or even multi-drug resistant) [6] microbes due to the overuse of antibiotics [7,8]. Furthermore, microbial colonization can subsequently lead to formation of

* Corresponding author.
E-mail address: Scheibel, T. (thomas.scheibel@bm.uni-bayreuth.de)
† These authors contributed equally to this work.

https://doi.org/10.1016/j.mattod.2020.06.009

almost irremovable biofilms, hardly accessible for antibiotics as, after becoming a dense colony, the microbes secrete a protective coating, making it much more difficult to eradicate biofilms in contrast to isolated microbes [9,10].

One example of a "superbug" is methicillin-resistant *Staphylococcus aureus*, a major cause of community-acquired infections resulting in high morbidity and mortality rates in hospital-acquired infections [11]. Concerning treatment of these infections, glycopeptide antibiotics (GPAs) targeting the acyl-D-alanyl-D-alanine (D-Ala-D-Ala) terminus of the growing peptidoglycans on the outer surface of the Gram-positive bacteria's cytoplasmatic membrane are considered the last, non-antibiotic resort for medical treatment [12]. Nevertheless, glycopeptide-resistant organisms cause new problems, as they significantly reduce antibiotic affinity by replacing the D-Ala-D-Ala terminus with D-alanyl-D-lactate (D-Ala-D-Lac) or D-alanyl-D-serine (D-Ala-D-Ser), prompting the search for second generation drugs and new strategies to inhibit spreading of such pathogens by new hygiene standards and for materials with explicit microbial repelling surfaces [13]. In this context, biomaterials with inherent non-fouling properties would provide new opportunities of long-term protection, especially when they can be used as surface coating materials for already existing products. However, one draw-back of such surfaces is that they often repel any kind of cells, even human ones, making it difficult to employ them in applications such as tissue engineering [14].

As one critical step in biofilm formation is the initial adherence of pathogenic microbes onto a material's surface [9], inhibiting microbial attachment is a favorable approach to develop material surfaces resistant to biofilm formation [15,16]. There are two main approaches for inhibiting surface attachment, referred to as either active or passive resistance. While passively resistant surfaces are typically made of super hydrophilic or hydrophobic as well as zwitterionic or other synthetic polymers [17–19], actively resistant ones are often "contact killing" materials, such as cationic polymers, amphiphilic polymers, antimicrobial peptides and polymeric/composite materials loaded with antimicrobial agents [20–25]. Although these approaches can combat microbial infection by inhibiting mechanisms of persistence and adaptation, several drawbacks exist, such as instability under physiological conditions, cytotoxicity to mammalian cells, inflammatory responses, a narrow antimicrobial spectrum, and implications for transmitting multidrug resistance [26]. Further, antimicrobial activity has been mostly investigated in terms of its effectiveness against bacteria, although fungal infections also contribute significantly to patient morbidity and mortality. Moreover, fungal infections can readily form polymicrobial biofilms with enhanced resistance to antifungal drugs, further limiting therapeutic options [27]. Therefore, efficient mitigation of microbial infection associated with both bacteria and fungi is required for the future development of broad-range multifunctional material coatings.

Spider silk exhibits extraordinary mechanical properties, surpassing the toughness of other polymer fibers, and further displays excellent biocompatibility useful for biomedical applications [28,29]. Remarkably, most spider silk webs withstand microbial omnipresence and remain resistant to microbial decomposition for years, irrespective of environmental impacts such as humidity, temperature, and location, though being composed of proteins and therefore of amino acids, which would be a valuable source of nutrition for microbes. Only few studies have been published examining microbe-repelling effects of natural spider silk [30], and so far, the underlying mechanism remains ambiguous. This is because the surface of silk fibers consists of varying mixtures of spidroins, glycoproteins and lipids, and the composition of the surface further depends on the spider species as well as environmental conditions [31]. In some cases, even antimicrobial peptides might be implemented in the spider silk coatings [32,33]. So far, the resistance of spider silk fibers against microbial infestation has only been macroscopically described, but not assigned to single material components such as lipids, glycoproteins, silk proteins or material features of these composite materials. Recently published results indicate that bacterial infestation and decomposition of spider silk is inhibited by bacteriostatic or microbe repellent properties rather than by antibacterial means [34,35]. The authors of this study further hypothesized, that the complex network of interconnected crystalline and non-crystalline structures might prevent accessibility of nitrogen, which is necessary for bacterial growth.

Here, 2D and 3D scaffolds based on explicit individual recombinant spider silk proteins, based on sequences of the dragline silk of the European garden spider *Araneus diadematus*, were found to withstand microbial infestation depending on the structural features of the material's surfaces. Two engineered *Araneus diadematus* fibroins eADF3 and eADF4 and variants thereof were utilized, based on consensus sequences of the core domains of the naturally occurring fibroins 3 and 4 [36,37]. Materials made of polyanionic eADF4(C16), the best investigated of these variants, display absence of toxicity, lack of immune reactivity and slow biodegradation [38,39]. As eADF4(C16) lacks cell binding motifs, like most so far identified spider silk proteins, eADF4(C16)-coated implants and catheters display significantly reduced adhesion and proliferation of mammalian cells as compared to non-treated ones [40,41]. When transplanted *in vivo* in rats, eADF4(C16)-coated silicone implants exhibited a substantial reduction in capsular fibrosis [40]. However, cell attachment to eADF4-based materials could be promoted by generating defined surface topographies, such as films with micrometer wide stripes or non-woven mats, on both of which good cell adhesion and proliferation could be detected due to the precisely controlled topography, dimensions and an increased surface area [42,43]. As a second approach, genetically modifying eADF4(C16) with the cell-binding motif RGD (Arginine-Glycine-Aspartate) promoted mammalian cell adhesion and proliferation with good cell viability in 2D and 3D materials [44,45]. Interestingly, even without sterilization, surfaces of materials based on the used recombinant spider silk protein eADF4(C16) were commonly free of microbes [46,34].

To systematically analyze microbe repellence, an extensive study was performed applying a diverse selection of different biofilm forming microbes, representing pathogenic bacteria (*S. mutans, S. aureus, E. coli*) and fungi/yeasts (*C. albicans, P. pastoris*) (Fig. 1a and Ref. [62]). Unlike the complex mixture/composite of natural spider silk fibers, recombinant technologies provide pure and perfectly defined proteins and materials made thereof, which are intrinsically non-toxic. Consequently, it was hypoth-

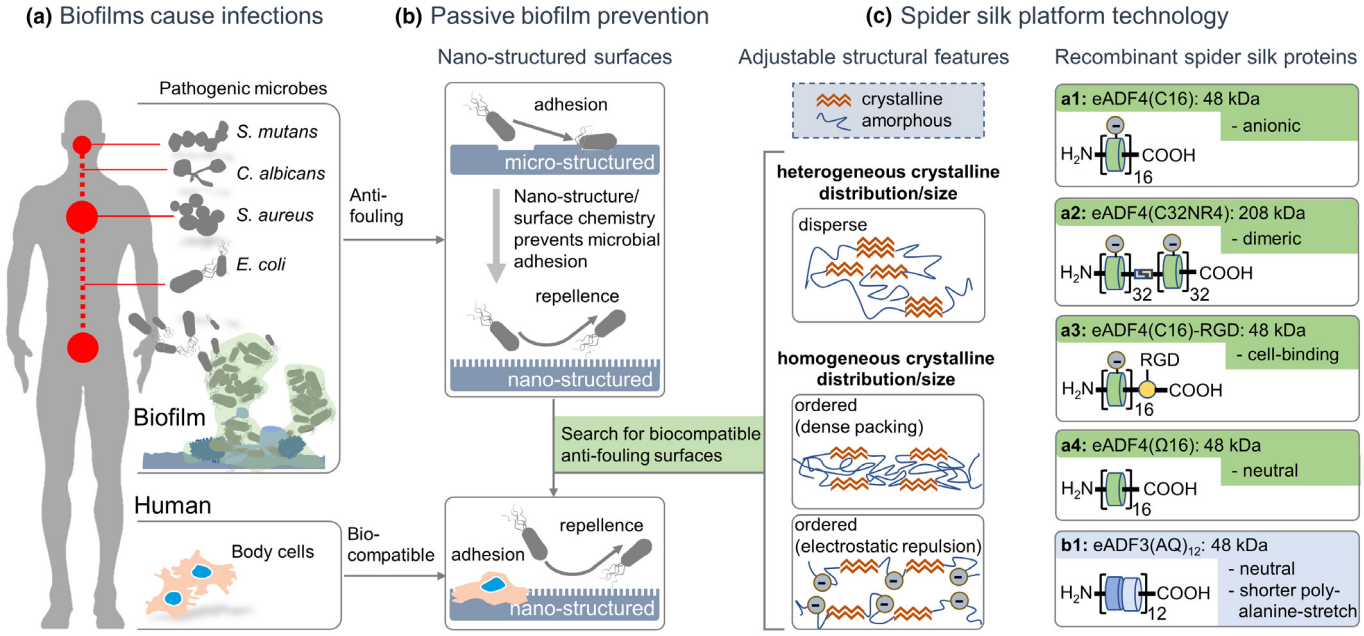

FIGURE 1

Schematic overview of the strategy to prevent biofilm formation using a spider silk platform technology. Various biofilm-forming microbes representing pathogenic bacteria and fungi as well as *P. pastoris* (model system) (a) were chosen to verify previously established concepts of passive biofilm prevention by nano-structured surfaces (b) using the established recombinant spider silk platform technology (c). It is predicted, as previously published, that particularly charge and amino acid sequence contribute to the homogeneity of crystallite size and distribution. Biotechnological engineering allows for systematic adaption of e.g. molecular weight (a1 vs. a2) and bio-functionality (a1 vs. a3) not affecting the crystallite properties of the underlying silk proteins. On the other hand, changes such as charge (a1 vs. a4) or amino acid sequence (a1 vs. b1) are expected to impact crystallite size and distribution. Combining microbe-repellant structural features with the ability to modify the intrinsically bio-compatible spider silk proteins with cell-adhesion motifs (a3) resulted in distinct bio-selective 2D and 3D spider silk materials.

esized, that anti-fouling effects of spider silk surfaces might not be attributed to toxic effects or explicit amino acid sequences, but to nano-structural features. Numerous technical [47,48] as well as natural [49,50] examples have shown the achievement of anti-fouling properties by nano-scaled topographies (Fig. 1b) [51]. Here, biotechnological design and recombinant production of different spider silk proteins was applied as a platform technology to systematically study the impact of the β-sheet structure-based nano-crystallites concerning anti-fouling performance (Fig. 1c). To test the hypothesis of nano-topographical effects leading to microbe-repellence, we investigated the impact of the bio-functionalization with a cell-binding motif (RGD), which doesn't change the basic crystallite-structural features of eADF4 (C16) and has the potential of supporting bio-selective mammalian cell growth with simultaneous microbe repellence (Fig. 1c: a1, a3). To evaluate the impact of molecular weight as well as terminal domains, eADF4(C32NR4) was included within this study as its non-repetitive terminal domain causes dimerization resulting in an apparent MW of 208 kDa (Fig. 1c: a2). As no structural differences between the core-domains of these proteins and that of eADF4(C16) could be detected [36], anti-fouling properties were expected to be the same.

On the other hand, structural changes and thus changed microbe-repellent properties were predicted to be induced by varying charges or different amino acid sequence motifs. To analyze the impact of charge, all negatively charged glutamic acid residues (E) in the consensus sequence of eADF4(C16) were replaced by uncharged glutamine residues (Q), resulting in the so far not examined neutral recombinant spider silk variant eADF4(Ω16) (Fig. 1c: a4). We predicted that loss of electrostatic repulsion would impact the homogeneous crystalline distribution as found in the eADF4(C16) structure leading to rather heterogenous packing, clustering, and distribution of β-sheet structures in eADF4(Ω16)-based materials. This feature could be already seen in self-assembly studies with much faster kinetics than that of the charged variant (data not shown). Although, the fibroin 3-based protein variant eADF3$(AQ)_{12}$ is also uncharged, the amino acid sequence significantly differs in length of the polyalanine as well as glycine-rich sequence motif with direct implications on β-sheet size/crystallite size as well as amorphous regions (Fig. 1c: b1). It is expected that the larger amorphous regions in eADF3$(AQ)_{12}$ sterically separate the crystal parts, leading to a more homogeneous distribution of crystals similar to those found in eADF4(C16), which are based on electrostatic repulsion (Fig. 1c: b1). This structural feature inhibits self-assembly into crystalline nanofibrils [36,52].

Importantly, recombinant spider silk proteins can be processed into solid morphologies such as films (representing the potential use as coatings of medical devices or bio-plastic foils as packaging materials) [41,53–56] or soft hydrogels (which are highly relevant in the fields of tissue engineering and biofabrication) [57–59]. Thus, the experimental design included the use of smooth and structured films as well as hydrogels. For comparison, regenerated *B. mori* fibroin was included representing a

non-spider silk type with a significantly different amino acid sequence and, respectively, slightly different structural features as well as crystal size, poly(caprolactone) (PCL) as a broadly applied biopolymer, and gelatin, a protein-based material which is often used in the context of tissue engineering and biofabrication (i.e. 3D-bioprinting together with cells) [60,61]. To explicitly analyze their suitability in the field of tissue engineering and biofabrication, the bio-selectivity of 2D and 3D materials made of recombinant spider silk proteins was tested in a post-operative contamination model including microbes and fibroblasts.

Results

Bacterial and fungal repellent properties of recombinant spider silk films

To systematically investigate the absence of microbes and the putative bacterial and fungal repellent properties of distinct spider silk surfaces, films of the negatively charged recombinant spider silk proteins eADF4(C16) and eADF4(C32NR4) and the uncharged eADF4(Ω16) and eADF3($(AQ)_{12}$) were fabricated to test the influence of the primary structure, molecular weight, net charge and the presence of a terminal assembly domain (see Table 1 in Ref. [62]) on microbial adhesion.

At first, we investigated biofilm formation on 2D-surfaces using *E. coli* and *P. pastoris*. Microbial viability was quantified using the CellTiter-Blue assay. The negligible adhesion of *E. coli* and *P. pastoris* on eADF4(C16), eADF4(C32NR4), and eADF3($(AQ)_{12}$) as well as eADF4(C16)-RGD films resulted in low fluorescence intensity in comparison to that of consolidated biofilm formation on eADF4(Ω16), *B. mori* fibroin and PCL films with much higher microbial viability (Fig. 2a). To the best of our knowledge, this bacterial and fungal repellent properties of materials made of recombinant spider silk are unique, and, as shown, even materials prepared from regenerated *B. mori* fibroin, which resemble to some extend the composition and properties of spider silk proteins but not at the amino acid sequence and nanostructural level, do not show such behavior.

Methicillin-resistant *Staphylococcus aureus* (MRSA) is a widespread problem in hospitals and is a highly infectious pathogen responsible for numerous fatalities worldwide. To investigate single bacterial adhesion forces of pathogens in contact with 2D spider silk surfaces, we used *S. aureus* which represents an established model organism for single cell adhesion tests. The forces involved in *S. aureus* adhesion on various film surfaces were previously quantified using atomic force microscopy (AFM) in force spectroscopy mode on single bacterial probes [63,64]. A single *S. aureus* cell was immobilized on a tipless AFM cantilever and pressed with a maximum force of 300 pN onto silanized glass slides coated with eADF4(C16), eADF4(C32NR4), eADF4(Ω16), eADF3($(AQ)_{12}$), *B. mori* fibroin, and PCL, the latter two acting as controls. Direct contact was allowed for some microseconds (termed 0 s in the following) or additional 5 s of surface delay time before the single bacterium was lifted and the adhesion force F_{ad} was measured. This contact time of several seconds is a simple method which has been previously established to investigate bacterial adhesion to various materials [65,66], and, therefore, the results obtained here could be directly compared to previous ones. The forces were normalized ($F_{ad\ (biopolymer\ coating)}$/ $F_{ad\ (silanized\ glass)}$), and the statistically

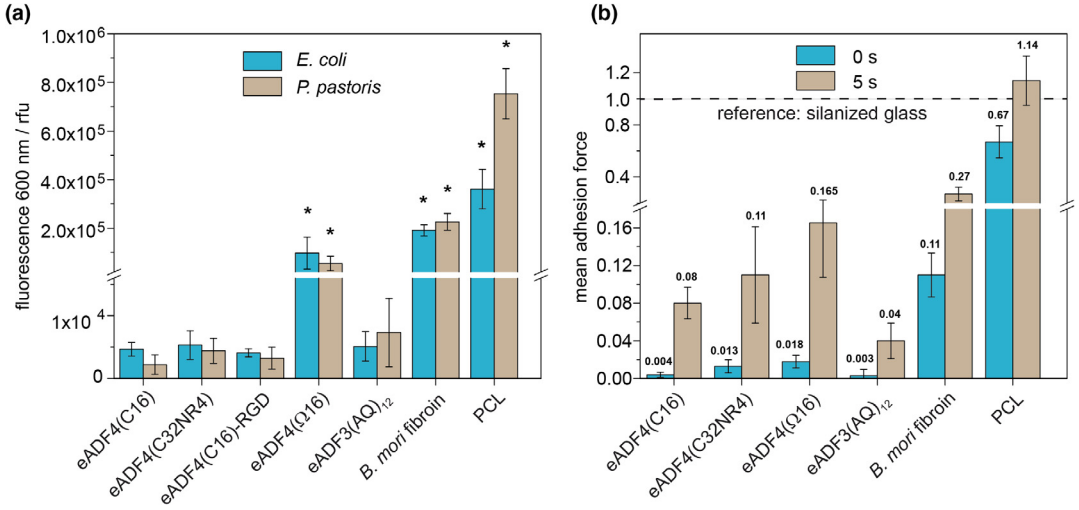

FIGURE 2

Bacterial and fungal repellent properties of 2D scaffolds made of recombinant spider silk proteins. (a) Viability of *E. coli* (blue) and *P. pastoris (brown) cells* on films of eADF4(C16), eADF4(C32NR4), eADF4(C16)-RGD, eADF3($(AQ)_{12}$), *B. mori* fibroin, and PCL, after incubation for 24 h at 37 °C. Microbial viability was quantified using the CellTiter-Blue assay by measuring the transformation of the blue fluorescent dye resazurin into red fluorescent resorufin using 530 nm excitation and 600 nm emission filters in a microplate reader. Each result is an average of five experiments, and the error bars designate the standard deviations. Student's t-test was performed for statistical analysis, * indicates significant difference to eADF4(C16) ($p < 0.05$). (b) Adhesion force measurements upon short contact using single *S. aureus* probes on silanized glass coated with eADF4(C16), eADF4(C32NR4), eADF4(Ω16), eADF3($(AQ)_{12}$), *B. mori* fibroin, and PCL, the latter two serving as controls. Representative normalized mean adhesion forces were obtained from 25 force-distance curves performed on each surface for 0 s (blue) as well as 5 s (brown) surface delay time using one and the same cell immobilized on a cantilever with a nominal spring constant of 0.03 N m^{-1}. Forces were referred to the values measured on uncoated silanized glass (4.8 ± 2.4 nN). It was detected that all distributions of adhesion forces were significantly different with p values below 0.001.

weighted mean adhesion force was determined. Thereby, the recombinant spider silk films made of eADF4(C16), eADF4(C32NR4), and eADF3($(AQ)_{12}$), yielded an extremely low bacterial adhesion force (Fig. 2b). The initial adhesive force at 0 s was slightly, but significantly higher on eADF4(Ω16) film surfaces (factor ~4.5) and even higher on surfaces of *B. mori* fibroin (factor ~28) and of PCL films (factor ~168) in comparison to that of eADF4(C16) films. At a surface delay time of 5 s, the adhesive forces increased in all cases, but still adhesion forces on the three recombinant spider silk protein-based films (eADF4(C16), eADF4(C32NR4), and eADF3$(AQ)_{12}$) were significantly lower than on the control materials (*B. mori* fibroin and PCL). These quantitative adhesion force measurements results of one model pathogen clearly indicated that explicit spider silk surfaces do not allow strong adhesion of *S. aureus* upon first contact while other surfaces do, an observation that is complementary to the biofilm formation assays made with the other bacteria and yeast strains.

This finding is intriguing, since the amino acid building blocks between the different silk proteins are similar with only slight differences. However, these differences are the basis of distinct structural features with significant impact on protein folding and e.g. fibril self-assembly [36,52]. The microbe-repellent properties of these different silks seem to be directly based on these structural features. To confirm that microbe-repellence is based on structural but not topographical features, flat spider silk films were compared to micro-patterned ones (2 μm wide grooves, 1 μm wide and 4 μm high ridges) concerning microbial adhesion. The surface topography of spider silk films has previously been shown to influence mammalian cell attachment and proliferation making this experiment important [42]. Suspended bacteria (*E. coli* and *S. mutans*) as well as fungi (*P. pastoris* and *C. albicans*) were seeded on top of all smooth and patterned films for 12 h at 37 °C (see also Ref. [62]). After washing to remove non-adherent microbes, films were air dried for microscopic analysis of microbial growth. Scanning electron microscope (SEM) images clearly showed that both smooth and patterned films of eADF3 and eADF4 variants (with the exception of eADF4(Ω16), Fig. 3d) substantially restricted the attachment, growth and microbial colonization of bacteria as well as fungi (Fig. 3a–c, e) and (Fig. 1 in Ref. [62]), and confirmed the superior repellence of spider silk 2D films as compared to *B. mori* fibroin and PCL (Fig. 3f and g). This finding confirmed the strict dependence of microbe adhesion to protein-structural surface pattern but not on surface topography, which was surprising since the grooves were expected to provide optimal niches for bacterial and fungal physical attachment, being thought to provide at least some impact on microbe adhesion. The microbe-repellence structural features were overruling any effect that the topography would normally have, which was also exhibited in the control groups. This property could have far-reaching impact on future applications, as for instance, *C. albicans* is an opportunistic, common fungal pathogen found in hospitals and is known to be highly infectious and life threatening.

Next, we investigated whether this protein structure-based bacterial and fungal repellent properties are restricted to the surface of explicit spider silk films or if they are generic, that is, the feature is retained when other spider silk morphologies (with identical protein structures) are prepared, such as hydrogels. Spider silk proteins can be processed into shear thinning hydrogels which can be 3D printed [45], and one possible application is their use as scaffolds in tissue regeneration. Therefore, bacterial and fungal repellent properties would complement other interesting features such as non-toxicity and biodegradability of recombinant spider silk hydrogels [38,39,55]. These properties, in combination with a controllable adhesion of mammalian cells, would boost their applicability in various biomedical applications, especially in biofabrication, i.e. the simultaneous printing of cells and materials (i.e. bioinks) for tissue regeneration [67].

Bacterial and fungal repellent properties of spider silk hydrogels

To monitor their bacterial and fungal repellent properties, spider silk hydrogels were incubated with *E. coli* and *P. pastoris* for 24 h at 37 °C. As a control, hydrogels of regenerated *B. mori* fibroin [68] and GelMA [69,70] as a further commonly used biomaterial were incubated in an identical manner. Subsequently, all hydrogels were washed carefully to remove non-adherent bacteria, and an alamar blue viability assay was used to determine *E. coli* and *P. pastoris* (see Ref. [62]). Spider silk hydrogels with microbes showed little alamar blue fluorescence, exemplarily shown for eADF4(C16) and eADF4(C16)-RGD (Fig. 4a) and (Fig. 2, Table 2, 3 in Ref. [62]). SEM images of lyophilized hydrogels clearly indicated that bacteria and fungi were not adhering and growing on and within recombinant spider silk hydrogels (Fig. 4b (i-ii) and c (i-ii)) even upon incubation for 10 days (Fig. 2, Table 2, 3 in Ref. [62]). Importantly, in this study, adhesion of microbial cells to eADF4(Ω16) hydrogels endorsed the microbe-repellence structural features of spider silk in 3D surfaces as well to some extent (Fig. 4d (i-ii)). It can be clearly seen that *B. mori* fibroin and GelMA hydrogels enabled *E. coli* and *P. pastoris* cells to adhere and colonize, and within both *B. mori* fibroin and GelMA hydrogels, microbial biofilms could be easily detected (Fig. 4e (i-ii) and f (i-ii)).

Bio-selective properties of spider silk films and hydrogels

Since the identified bacterial and fungal repellent properties of distinct spider silk materials can be distinguished from the previously determined topography-dependent adhesion of mammalian cells, we wanted to elucidate whether it is possible to trigger a bio-selective behavior, which represses the growth of microbes but enhances mammalian cell attachment and proliferation on spider silk materials. To improve mammalian cell adhesion, we used eADF4(C16)-RGD known to interact with integrin receptors to promote mammalian cell attachment [44,45,58]. Importantly, all other physicochemical characteristics of this variant are indistinguishable to that of eADF4(C16) including pronounced bacterial and fungal repellent properties to resist biofilm formation as shown above.

Hydrogels made of eADF4(C16) and eADF4(C16)-RGD were used to encapsulate BALB/3T3 fibroblasts yielding bioinks for biofabrication and were then inoculated with *E. coli* and *P. pastoris* for 6 h to mimic a situation similar to that of a tissue regeneration scenario as found for post-operative infection (Fig. 3 in Ref. [62]). After 6 h of incubation, hydrogels were washed carefully to remove non-adherent cells (mammalian as well as microbial), and the hydrogels were further incubated with fresh cell

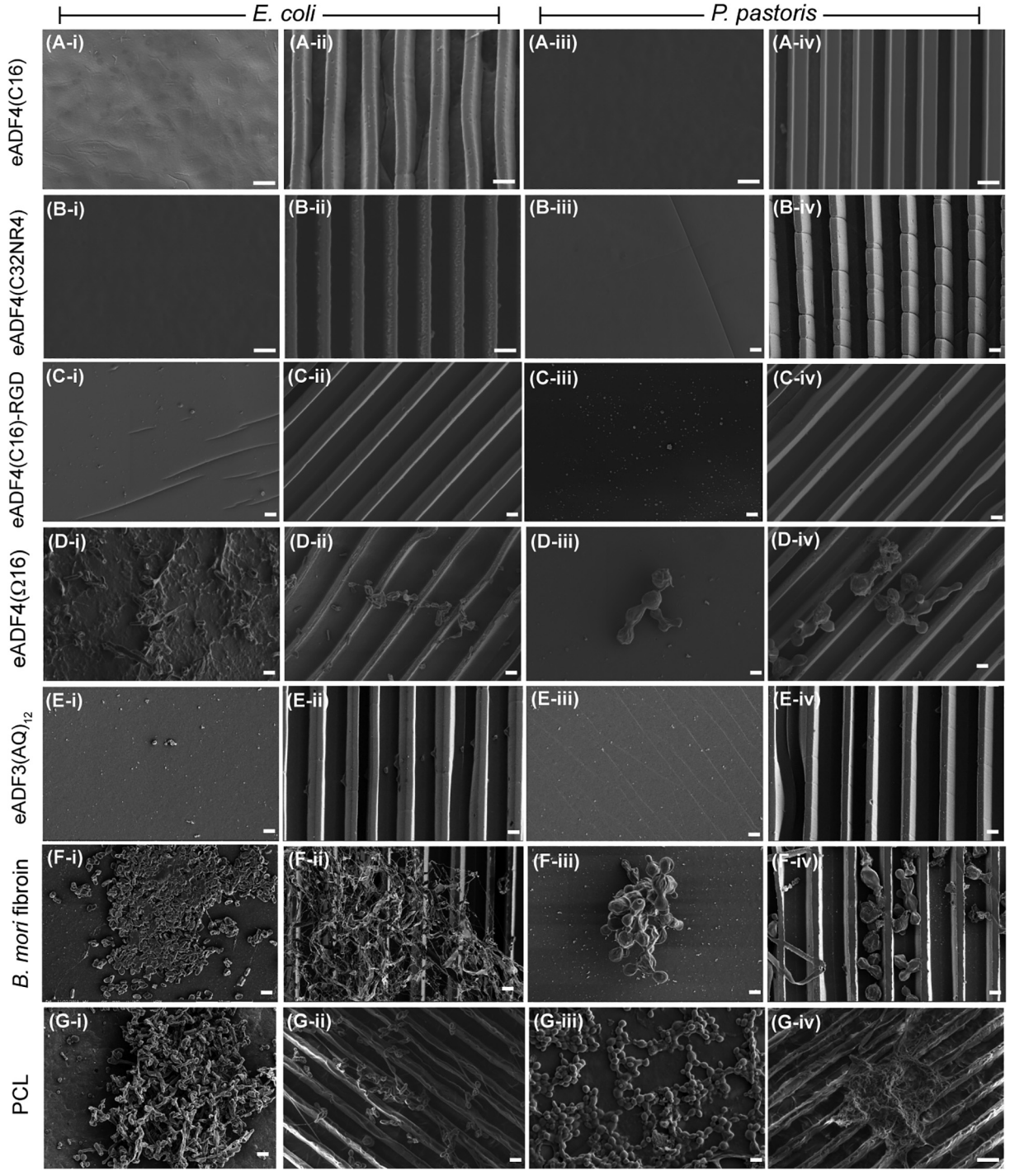

FIGURE 3

Bacterial and fungal repellent properties of films made of recombinant spider silk proteins. SEM images showing (i & iii) plane and (ii & iv) micro-patterned surfaces of films made of (a) eADF4(C16), (b) eADF4(C32NR4), (c) eADF4(C16)-RGD, (d) eADF4(Ω16), (e) eADF3$(AQ)_{12}$, (f) *B. mori* fibroin and (g) PCL after 12 h of incubation with (i & ii) *E. coli* and (iii & iv) *P. pastoris* at 37 °C. Scale bars = 2 μm.

culture media. Viability of microbes and fibroblasts was evaluated by microscopy and live/dead staining after 3, 6, and 10 days of incubation (Fig. 5a–d). Encapsulated fibroblasts showed good viability within the hydrogels made of eADF4(C16) and eADF4(C16)-RGD over a culture period of 10 days (Fig. 5e), while no bacterial and fungi growth/contamination could be detected during the entire cultivation period (Fig. 5f and g), since the microbes could not adhere to the hydrogels to start colony formation and did not manifest a biofilm. As expected, introduction of the RGD-sequence stimulated the proliferation of BALB/3T3 fibroblasts in contrast to eADF4(C16) hydrogels in which very little proliferation was observed.

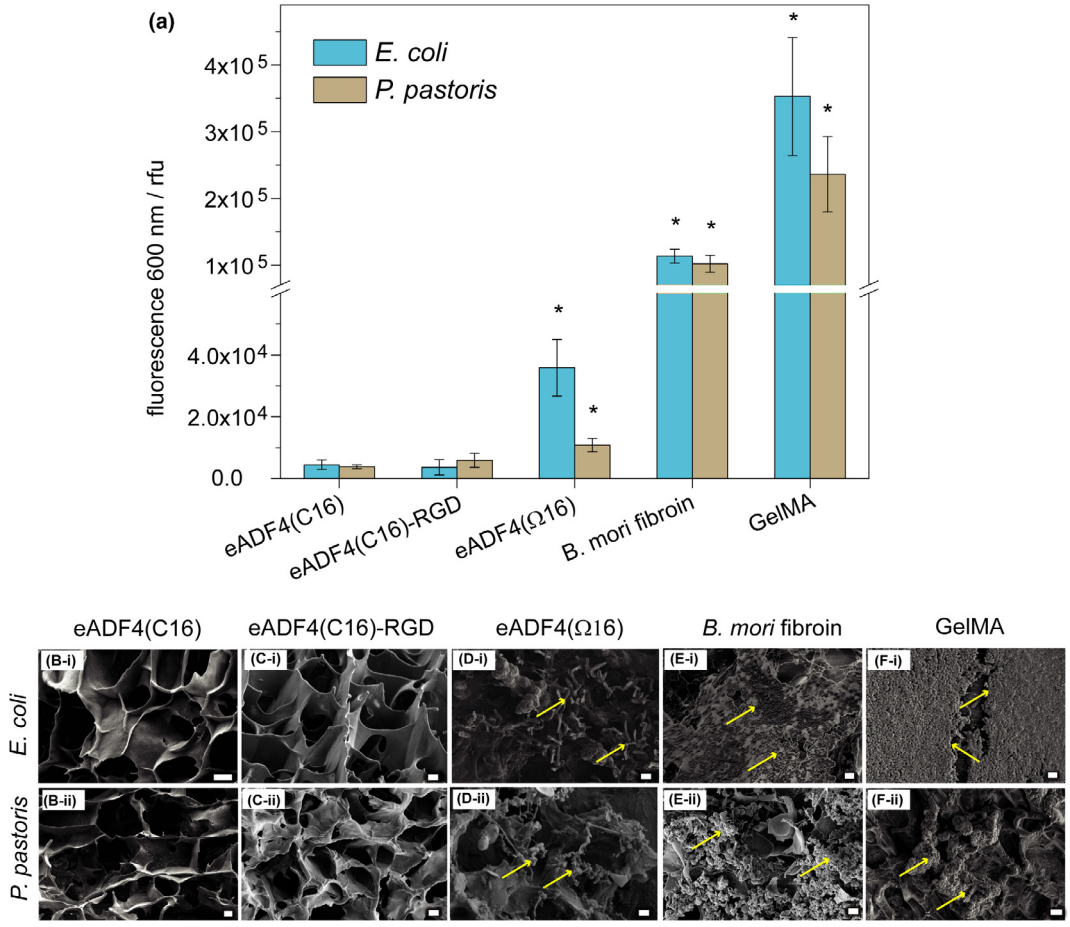

FIGURE 4

Bacterial and fungal repellent properties of spider silk and other hydrogels. (a) Viability of microbial cells on hydrogels made of eADF4(C16), eADF4(C16)-RGD, eADF4(Ω16), *B. mori* fibroin and GelMA after 24 h incubation with *E. coli* and *P. pastoris* at 37 °C. Microbial viability was quantified using the alamar blue assay by measuring the transformation of the blue fluorescent dye resazurin into red fluorescent resorufin with 530 nm excitation and 600 nm emission filters in a microplate reader. Minimal adhesion of *E. coli* and *P. pastoris* on eADF4(C16) and eADF4(C16)-RGD hydrogels resulted in low fluorescence intensity in comparison to adhesion on eADF4(Ω16), *B. mori* fibroin and GelMA hydrogels with higher microbial viability. Each result is an average of three experiments, and the error bars designate the standard deviations. Student's *t*-test was performed for statistical analysis, *indicates significant difference to eADF4(C16) ($p < 0.05$). SEM images of hydrogels prepared from (b) eADF4(C16), (c) eADF4(C16)-RGD, (d) eADF4(Ω16), (e) *B. mori* fibroin and (f) GelMA after 24 h of incubation with (i) *E. coli* and (ii) *P. pastoris*. Arrows show biofilm or microbial cells on hydrogels. Scale bars = 2 μm.

Discussion

Microbial adhesion tests with different pathogenic microorganisms using both bacteria (*S. mutans, S. aureus,* and *E. coli*) and fungi (*C. albicans,* and *P. pastoris*) demonstrated microbe repellence of distinct recombinant spider silk materials. None of the tested microbes could manifest biofilms on selected recombinant spider silk films, hydrogel surfaces or within hydrogels. The inherent property of bacterial and fungal repellent performance of distinct spider silk materials is related to the structural features of the underlying proteins responsible for the formation of hydrophobic patches [52,71]. The used protein platform technology (Fig. 6a), confirmed the correlation of adhesion of microorganisms with the presence of hydrophobic patches (Fig. 6b, and c). As shown schematically, based on the primary sequence, hydrophobic patches can be engineered due to either intermolecular charge-charge repulsion as in eADF4(C16) and eADF4 (C32NR4) or a volume effect of the amorphous region in eADF3 $(AQ)_{12}$. In contrast, the absence of charge in eADF4(Ω16) induces a denser and less homogeneous packing of nano ß-crystallites, creating new anchoring sites for microbes. On the mesoscale, microbial cell attachment most readily occurs on surfaces which are rougher, more hydrophobic, and positively charged. Distinct silk proteins, such as spider silk and silkworm silk, feature structural differences e.g. concerning the β-sheet crystallite size (spider silk: ~7 nm, *B. mori* fibroin ~14–200 nm) and crystallite orientation [54,72,73], both influencing the dimensions of the respective hydrophobic patches. Our study demonstrated that 2D and 3D surfaces of *B. mori* fibroin with larger hydrophobic patches than that of spider silk are easily accessible for microbial manifestation. Finally, RGD-modified spider silk with homogeneous hydrophobic patches showed repellence of microbes but allowed selective mammalian cell adhesion and proliferation.

In comparison to natural spider silk with its composite surface layer, it is highly interesting that no additional components such as glycoproteins, lipids or antimicrobial agents but only the structural features of individual recombinant spider silk proteins

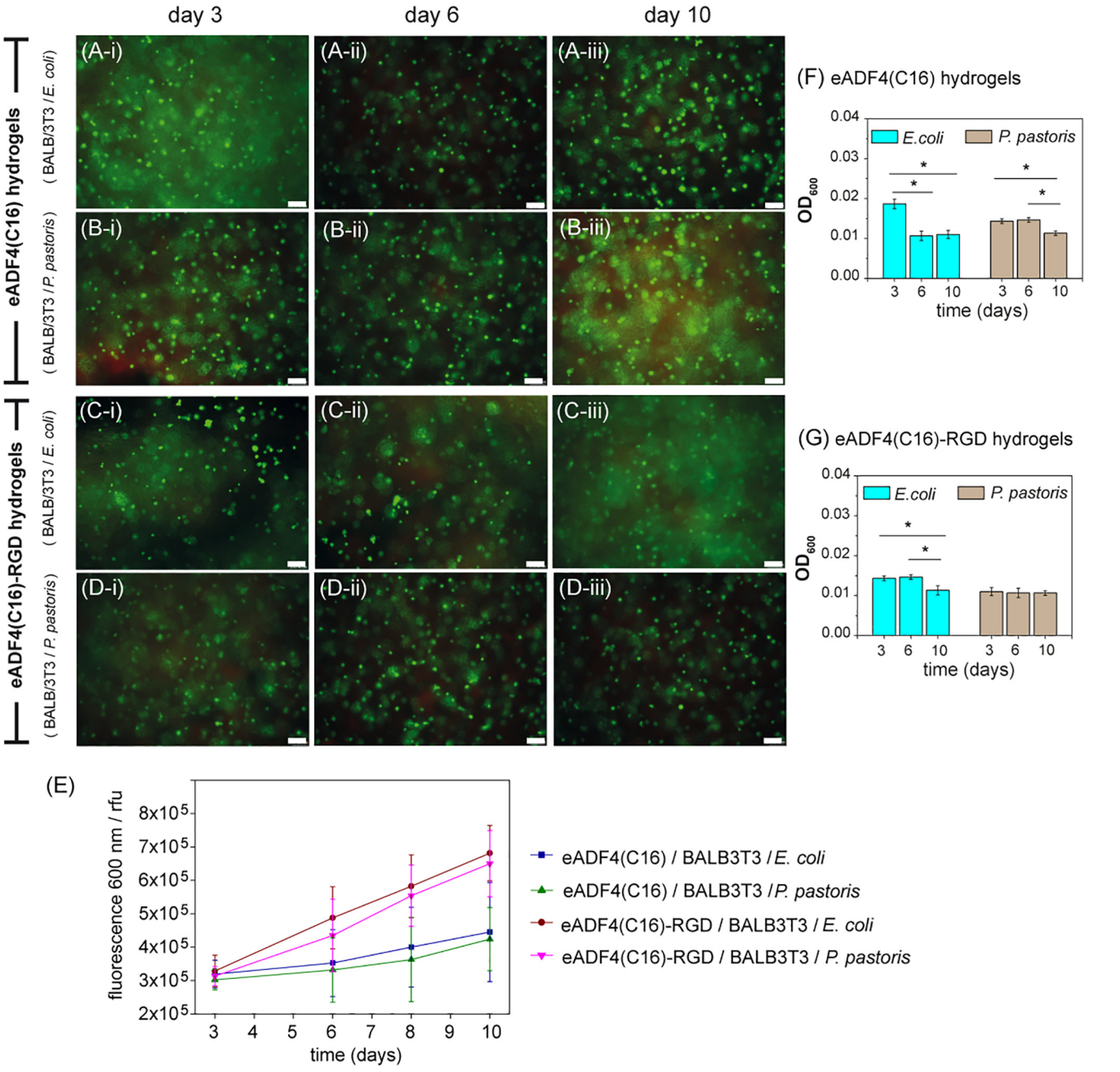

FIGURE 5

Bacterial and fungal repellent properties of 3D scaffolds made of eADF4(C16) and eADF4(C16)-RGD in a post-operative contamination model containing microbes and mammalian cells. Fluorescence images of (a and b) eADF4(C16) and (c and d) eADF4(C16)-RGD hydrogels with encapsulated BALB/3T3 fibroblasts (i.e. bioinks for biofabrication) and cultured with (a and c) *E. coli* and (b and d) *P. pastoris* for (i) 3 days, (ii) 6 days, and (iii) 10 days. Scale bars = 100 μm. The cells were stained with calcein A/M (live cells: green) and ethidium homo dimer I (dead cells: red). Ethidium homodimer I also stained the hydrogels yielding an unspecific red background fluorescence (a–d). Proliferation of mouse fibroblasts (BALB/3T3) in presence of microbes was measured over 10 days using (e) the absorbance of cell titer blue. Microbial growth of *E. coli* and *P. pastoris* in fresh media was measured using (f and g) optical density at 600 nm (OD_{600}) with microbial inoculated hydrogels (after washing) and after incubation for 12 h at 37 °C. Each result is an average of three experiments and the error bars designate the standard deviation. Student's *t*-test was performed for statistical analysis, $*p < 0.05$.

are necessary to generate a microbe-repellent spider silk surface. To the best of our knowledge, this is a completely new finding which opens the door for novel applications of spider silk materials, e.g., as bioselective coatings in various biomedical applications as for the preparation of bioinks for biofabrication and regeneration medicine.

Methods

Protein design and production of recombinant spider silk proteins: eADF4(C16) was purchased from AMSilk GmbH (Planegg, Germany). The recombinant spider silk proteins eADF4(C16)-RGD, eADF4(C32NR4) and $eADF3(AQ)_{12}$ were produced and purified as described previously [36,44]. To generate the uncharged

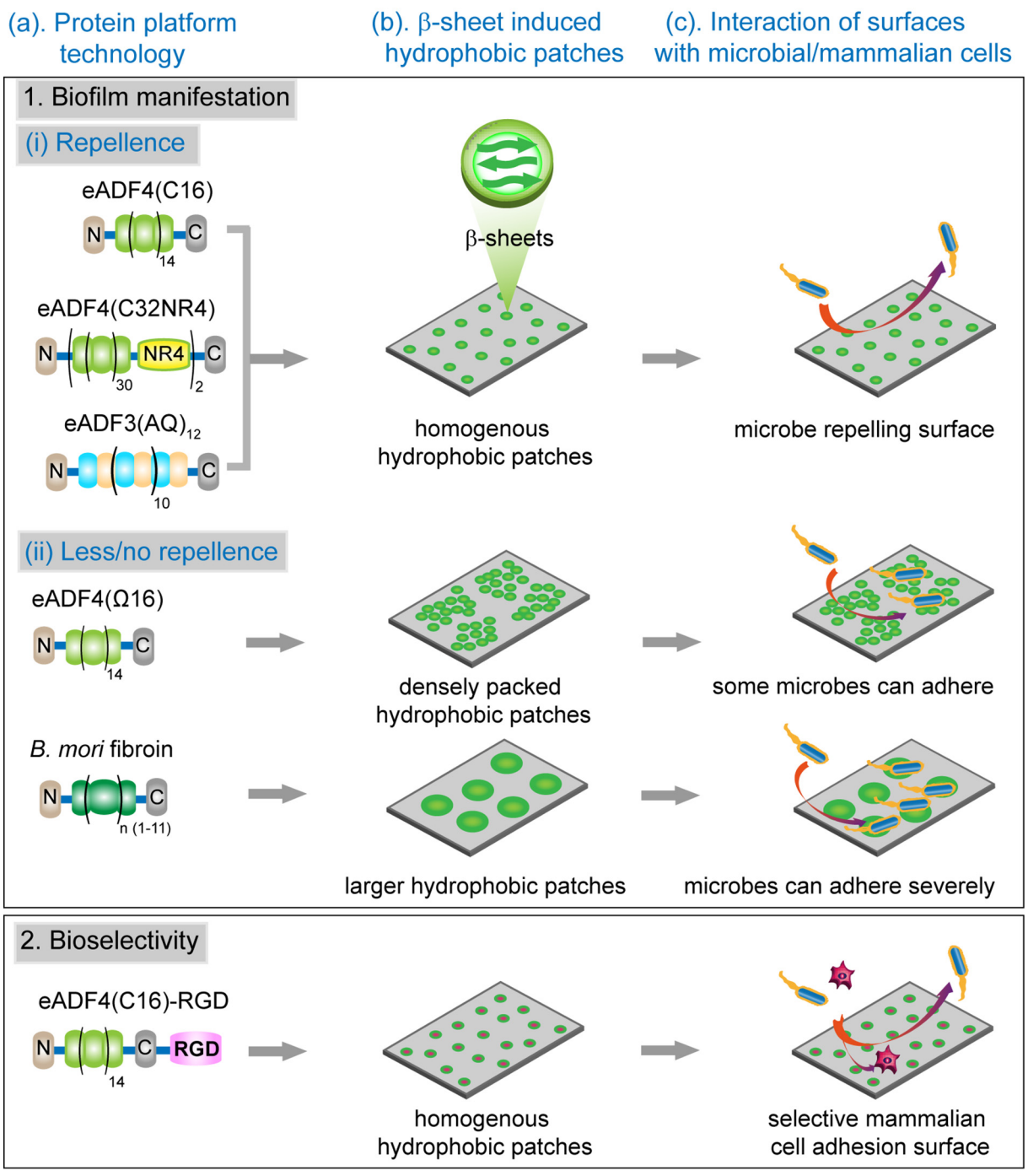

FIGURE 6

Schematic illustration of the microbial behavior on silk materials with (1) repellent/non-repellent and (2) bioselective surfaces. (a) Recombinant spider silk variant/silkworm silk, (b) β-sheet formation yields hydrophobic surface patches with unique distribution and dimensions. (c) Homogeneous hydrophobic patch distribution of eADF4(C16), dimeric eADF4(C32NR4), and eADF3($(AQ)_{12}$) shows microbe repellence characteristics. The absence of charge-charge repulsion or steric effects in eADF4(Ω16) leads to dense packing of hydrophobic patches and structured larger hydrophobic patches in *B. mori* fibroin favoring the attachment of microbial cells. eADF4(C16)-RGD allows selective mammalian cell attachment with simultaneous microbe repellence.

eADF4(Ω16) variant, the glutamic acid residues (E) of the consensus sequence of eADF4(C16) were exchanged with glutamine (Q) ones. The recombinant spider silk protein eADF4(Ω16) was produced in *E. coli* BL21 gold (DE3) and purified following a protocol as described previously [36]. Briefly, after cell disruption eADF4 (Ω16) was purified using a heat step and an ammonium sulphate precipitation.

Bombyx mori (B. mori) fibroin protein: Regenerated fibroin solutions were prepared as described previously [68] by dissolving degummed (boiled for 30 min in 0.02 M sodium carbonate) silk fibres in 9.3 M LiBr solution, dialysis against ultrapure water (Milli-Q) for 2 d at 4 °C, centrifugation at 8500 rpm for 45 min at 4 °C, and collection of the supernatant. The *B. mori* fibroin solutions had a final concentration of ~6% w/v and were stored

at 4 °C until use. To produce flat and patterned films, solutions were freeze-dried and processed in the same way as spider silk and PCL.

Production of flat and patterned films: All flat and patterned films of proteins and polycaprolactone (PCL; Perstorp AB) were produced by film casting onto patterned polydimethylsiloxane (PDMS; Sylgard 184 Silicone Elastomer, Dow Corning) substrates. PDMS stamps were produced by casting of a 10:1 mixture of PDMS pre-polymer and curing agent (degassed for 20 min) on a photo-lithographically patterned waver to generate the desired geometry (12 × 12 mm area with 2 μm wide grooves, ridges with a width of 1 μm and a height of 4 μm). After curing at 80 °C for 90 min, the stamps were solidified and could be easily peeled off. To produce patterned films, proteins and PCL were dissolved in 1,1,1,3,3,3,-hexafluoro-2-propanol (HFIP; Alpha Aesar) at a concentration of 100 mg/mL (room temperature, overnight). To generate films with a thickness of 10–15 μm, 250 μL of solution (corresponding to 25 mg of protein/polymer) were poured into the stamp, and the solvent was subsequently evaporated at room temperature. The dried patterned films were removed and post-treated with 100% ethanol for 1 h to render the silk protein water insoluble upon induction of β-sheet structures. To ensure that only material properties determined the results of microbial growth experiments, all samples (including PCL films) were treated the same way. After post-treatment, the samples were stored sterile in 70% ethanol at 4 °C.

Bacteria and yeast culture on films: *Streptococcus mutans* (DSMZ 20523, Braunschweig) and *Candida albicans* (patient isolate), stored at −80 °C, were thawed at RT, fractionally spread on Columbia blood agar (PB 5039A, oxoid, Wesel) and incubated for 48 h at 37 °C and 5% CO_2. Afterwards, an overnight culture was prepared in BBLTM Schaedler Broth medium (Becton Dickinson, Sparks MD, USA), and then the culture was diluted (1:10) with Schaedler Broth medium (see also Ref [62]).

Escherichia coli BL21(DE3)-gold (Novagen, Merck, Darmstadt, Germany), stored at −80 °C, was thawed at RT and inoculated in Luria–Bertani medium (LB), at 37 °C with constant shaking at 150 rpm until an optical density (OD_{600}) between 0.8 and 1 was reached (corresponding to a viable count of approx. 10^7–10^8 CFU mL^{-1}). The *E. coli* culture was diluted (1:10) with LB medium.

Pichia pastoris X33 (wild type, Invitrogen, Germany) was inoculated in YPD-media and allowed to grow for 24 h at 30 °C with constant shaking at 150 rpm. The *P. pastoris* culture was diluted (1:10) with YPD medium.

Staphylococcus aureus (strain SA113), stored at −20 °C, was thawed and cultured on blood agar plates for three days at 37 °C. Then, one colony from a plate was transferred into 5 mL of sterile tryptic soy broth (TSB) and cultured overnight at 150 rpm, 37 °C. For each experiment, 40 μL of the culture were transferred into 4 mL fresh TSB and cultured for another 2.5 h at 37 °C. The bacterial culture was washed three times with sterile phosphate buffered saline (PBS). The final suspension of bacteria in PBS was stored at 4 °C and used no longer than 6 h.

Silk and polymer films were taken out of 70% ethanol, subsequently washed with PBS (8.18 g NaCl, 0.2 g KCl, 0.24 g anhydrous KH_2PO_4, 1.78 g $Na_2HPO_4 \times 2H_2O$, 1 L distilled water, pH 7.4, Sigma Aldrich, St. Louis, Missouri, USA), and incubated in 5 mL of diluted microbial solution (as described above) in petri dishes (Φ 5 cm) for 60 h (5% CO_2, 37 °C). Then, the films were removed and carefully washed with PBS to remove non-adherent bacteria and yeast cells and dried at room temperature for subsequent SEM imaging.

Adhesion force measurements: A single *S. aureus* cell was attached to a tipless AFM cantilever (MLCT-0 with a nominal spring constant of 0.03 N/m from Bruker Nano, Santa Barbara, Ca, USA) coated with polydopamine that was calibrated before each set of experiments [63,64]. Force-distance measurements were performed using a Bioscope Catalyst from Bruker-Nano in PBS at room temperature. The maximum force with which the cell was pressed onto the surfaces was set to 300 pN. On each surface, 25 force-distance curves were performed for 0 s and 5 s of additional surface delay time with one and the same cell, the total number of individual cells being twelve. The results obtained from three of these cells were not used for the analysis as their adhesion forces were less than 5% of the mean adhesion force of the remaining cells indicating that the adhesive strengths of these cells were not representative for the totality of *S. aureus* cells used. Nine more cells were tested on eADF4 (C16), *B. mori* fibroin, and PCL with identical parameters under the same conditions. Approaching speed towards the surfaces was set to 800 nm/s for 0 s of surface delay time and 100 nm/s for 5 s of surface delay time. Retraction speed was 800 nm/s. To test the results of adhesion measurements for statistical significance, all adhesion force distributions were analyzed in pairs by a Man–Whitney-*U*-test with the software Matlab.

Bacterial and yeast cell viability: Adhesion of *E. coli* and *P. pastoris* to silk and polymer films or hydrogels was measured by analysis of cell vitality using the CellTiter-Blue assay after culturing for 24 h at 37 °C. Samples incubated with bacterial and yeast cells were washed with phosphate buffered saline (PBS; Sigma-Aldrich) three times, and then incubated with 10% CellTiter-Blue (Promega) in PBS for 3 h at 37 °C. Transformation of the blue fluorescent dye resazurin into red fluorescent resorufin (λ_{ex} = 530 nm; λ_{em} = 590 - nm) was measured using a plate reader (Mithras LB 940, Berthold, Bad Wildbad) with a counting time of 0.5 s.

Preparation of eADF4(C16), eADF4(C16)-RGD and eADF4(Ω16) hydrogels: Lyophilized eADF4(C16) and eADF4(C16)-RGD were dissolved in 6 M guanidinium thiocyanate (GdmSCN) at 5 mg/mL and dialyzed using dialysis membranes with a molecular weight cutoff of 6–8 kDa against 10 mM Tris/HCl, pH 7.5 overnight at room temperature. Subsequent dialysis against 20% w/v poly (ethylene glycol) (PEG, 20,000 g/mol) at a volume ratio of PEG/eADF4(C16) solution of 100:1 was used to remove water by osmotic pressure and to adjust 30 mg/mL (3% w/v) spider silk solutions. Hydrogels were self-assembled after an overnight incubation at 37 °C. For the preparation of eADF4(Ω16) hydrogels, due to the faster self-assembly of fibrils, all steps were carried out at 4 °C, and hydrogels were prepared at a concentration of 20 mg/mL (2% w/v).

For post-operative contamination experiments, 1×10^6 BALB/3T3 fibroblasts were added to 3% w/v eADF4(C16) and eADF4(C16)-RGD spider silk solutions before gelation in an incubator at 37 °C.

Preparation of B. mori fibroin hydrogels: *B. mori* fibroin hydrogels were prepared using sonication-induced gelation, as previously reported [68]. In brief, 4% (w/v) aqueous silk fibroin solution in a 15 mL conical tube was ultra-sonicated (Ultrasonic Homogenizers HD 3100, BANDELIN) at 50% amplitude (21 W) for 30 s, and overnight incubation at 37 °C induced gelation.

Preparation of methacrylated gelatin hydrogels: Gelatin Methacrylate (GelMA) was produced upon reacting gelatin solutions (gelatin from bovine skin, Type B, ~225 g Bloom, Sigma-Aldrich) with methacrylic anhydride (Sigma-Aldrich) following previously described protocols [69,70]. After the dissolution of 10% (w/v) gelatin in 0.1 M CB buffer (3.18 g sodium carbonate and 5.86 g sodium bicarbonate in 1L distilled water) at 60 °C, one sixth of 1% (v/v) methacrylic anhydride was added dropwise every 30 min for 3 h. The solution was vigorously stirred for another 1 h, diluted with 0.1M CB, and dialyzed for 2 days against ultrapure (Milli-Q) water at 37 °C. The solution was then freeze-dried in a lyophilizer to obtain methacrylamide-modified gelatin as a dry white powder.

Methacrylamide-modified gelatin hydrogel was obtained by UV exposure of 5% (w/v) GelMA solution in 24 well cell culture vessels at 365 nm using an ultraviolet lamp (Benda, type NU -4 KL) for 15 min in the presence of 0.5 mg/mL of the photoinitiator 2-hydroxy-4′-(2-hydroxyethoxy)-2-methylpropiophenone (Irgacure- 2959, Sigma-Aldrich).

Bacteria and yeast culture with hydrogels: Hydrogels were incubated with 1 mL of diluted liquid cultures of *E. coli* and *P. pastoris* for 12 h at 37 °C. Hydrogels were washed with phosphate buffered saline (PBS; Sigma-Aldrich) three times to remove non-adherent bacteria and yeast cells and then lyophilized.

Microbial adhesion: The microbe repellence activity of eADF4 (C16) and eADF4(C16)-RGD hydrogels concerning *E. coli* and *P. pastoris* was measured by inoculating the supernatant (100 μL) of the microbe-treated hydrogels (after washing) in fresh media and culturing for additional 12 h at 37 °C. Optical density at 600 nm (OD_{600}; OD600 DiluPhotometer™, IMPLEN) was measured to monitor microbial growth/infection.

BALB/3T3 cultivation: BALB/3T3 mouse fibroblasts (European Collection of Cell Cultures) were cultured in Dulbecco's Modified Eagle Medium (DMEM, Biochrom) supplemented with 10% fetal bovine serum (Biochrom) and 1% (v/v) GlutaMAX (Gibco) in a controlled atmosphere of 5% CO_2, 95% humidity and at 37 °C. Viability and number of cells were analyzed using trypan blue (Sigma-Aldrich) in a Neubauer chamber (Laboroptik, UK).

Post-operative contamination model: eADF4(C16) and eADF4 (C16)-RGD hydrogels with encapsulated BALB/3T3 mouse fibroblasts (i.e. bioinks) were prepared in hanging cell culture inserts using 24-well plates (Merck Millipore) and then exposed to diluted (1:10, corresponding to OD 0.25) bacterial and yeast cells prepared in DMEM for 6 h at 37 °C and 80% relative humidity. Hydrogels were washed three times to remove non-adherent microbes and incubated with fresh DMEM media and cultivated for 10 days under identical conditions. Cell culture medium was changed every 24 h. The cell viability of BALB/3T3 mouse fibroblasts was analyzed using a Live/Dead assay after 3, 6 and 10 days.

Live/Dead assay: Films and hydrogels of eADF4(C16) and eADF4(C16)-RGD were washed with PBS and stained with Calcein acetoxymethylester (Calcein A/M, Invitrogen) and Ethidium Homodimer-1 (EthD-1, Invitrogen) in cell culture medium for the detection of live and dead cells, respectively. Calcein A/M was added to the medium at a final concentration of 0.3 μM, and Ethidium Homodimer-1 was added to the medium at a final concentration of 0.1 μM and incubated for 30 min. After staining, the solution was removed, and fresh PBS was added for imaging. Live and dead cells were visualized and analyzed using a fluorescence microscope (Leica DMi8, Wetzlar) and processed using either Leica Application Suite or Image J.

Scanning electron microscopy (SEM): To analyze the morphological structure using SEM, hydrogels were lyophilized and fixed to SEM stubs using conductive carbon cement solution (Leit-C, PLANO GmbH). Samples were sputter-coated with 2 nm platinum (Sputter Coater 208 HR with 268 MTM 20, Cressington, Watford, U.K.) and then imaged at an accelerating voltage of 2.5 kV using a scanning electron microscope 270 Zeiss Sigma VP 300 (Zeiss, Oberkochen, Germany) and Field Emission Gun (FEG; Apreo VS, ThermoFisher Scientific/FEI, Germany).

CRediT authorship contribution statement

Sushma Kumari: Conceptualization, Methodology, Validation, Formal analysis, Investigation, Data curation, Writing - original draft, Writing - review & editing, Visualization. **Gregor Lang:** Conceptualization, Methodology, Validation, Formal analysis, Investigation, Data curation, Writing - original draft, Writing - review & editing, Visualization. **Elise DeSimone:** Methodology, Formal analysis, Investigation, Data curation, Writing - review & editing. **Christian Spengler:** Methodology, Validation, Formal analysis, Investigation, Data curation. **Vanessa T. Trossmann:** Methodology, Validation, Formal analysis, Investigation, Data curation, Writing - review & editing. **Susanne Lücker:** Methodology, Validation, Formal analysis, Investigation, Data curation. **Martina Hudel:** Methodology, Validation, Formal analysis, Investigation, Data curation. **Karin Jacobs:** Supervision, Funding acquisition, Writing - review & editing. **Norbert Krämer:** Supervision, Writing - review & editing. **Thomas Scheibel:** Conceptualization, Supervision, Funding acquisition, Writing - review & editing.

Declaration of Competing Interest

The authors declare that they have no known competing financial interests or personal relationships that could have appeared to influence the work reported in this paper.

Acknowledgements

The authors thank Dr. Hendrik Bargel for SEM imaging. This project has been funded by the Deutsche Forschungsgemeinschaft (DFG, German Research Foundation)-project number 326998133–TRR225 (funded subprojects and PIs: A07: G.L.; C01: T.S.and JA 905/6: C. S.) as well as SFB840 (A08: T.S.) and SFB 1027 (B2: K.J.).

Author contributions

S.K. and G.L. contributed equally to this work. S.K. performed the in vitro bacterial/ fungal repellent experiments and coculture experiments on films and hydrogels with *E. coli* and *P. pastoris*. G. L. prepared films (smooth and patterned), prepared protein

coated silanized glass slides, performed SEM and analyzed the data. E.D. assisted in designing of coculture experiments. V.T.T. designed, synthesized, and purified the recombinant spider silk variant eADF4(Ω16) and assisted in handing of the protein. S. L., M.H. and N.K. carried out in vitro experiments of *S. mutans* and *C. albicans*. C.S. and K.J. prepared bacterial probes and performed force distance measurements. T.S. designed the experiments and supervised the project. S.K. and G.L wrote the manuscript. E.D., V.T.T., C.S., K.J. and T.S. contributed to writing and editing of the manuscript.

Competing interests

The authors declare the following competing financial interest (s): T.S. is co-founder and shareholder of AMSilk GmbH.

References

[1] L.L. Leape et al., The Nature of adverse events in hospitalized patients, N. Engl. J. Med. 324 (1991) 377–384. http://www.nejm.org/doi/full/10.1056/NEJM199102073240605.

[2] V. Russotto et al., Bacterial contamination of inanimate surfaces and equipment in the intensive care unit, J. Intensive Care 3 (2015) 54, https://doi.org/10.1186/s40560-015-0120-5.

[3] A. Gristina, Biomaterial-centered infection: microbial adhesion versus tissue integration, Science 237 (1987) 1588–1595, https://doi.org/10.1126/science.3629258.

[4] E. Barth et al., In vitro and in vivo comparative colonization of Staphylococcus aureus and Staphylococcus epidermidis on orthopaedic implant materials, Biomaterials 10 (1989) 325–328, https://doi.org/10.1016/0142-9612(89)90073-2.

[5] B. Carpentier, O. Cerf, Biofilms and their consequences, with particular reference to hygiene in the food industry, J. Appl. Bacteriol. 75 (1993) 499–511, https://doi.org/10.1111/j.1365-2672.1993.tb01587.x.

[6] S.B. Levy, B. Marshall, Antibacterial resistance worldwide: causes, challenges and responses, Nat. Med. 10 (2004) S122–S129, https://doi.org/10.1038/nm1145.

[7] D. Davies, Understanding biofilm resistance to antibacterial agents, Nat. Rev. Drug Discov. 2 (2003) 114–122, https://doi.org/10.1038/nrd1008.

[8] G.D. Wright, The antibiotic resistome: the nexus of chemical and genetic diversity, Nat. Rev. Microbiol. 5 (2007) 175–186, https://doi.org/10.1038/nrmicro1614.

[9] J.W. Costerton, P.S. Stewart, E.P. Greenberg, Bacterial biofilms: a common cause of persistent infections, Science 284 (1999) 1318–1322, https://doi.org/10.1172/JCI23825.

[10] P.S. Stewart, J. William Costerton, Antibiotic resistance of bacteria in biofilms, Lancet 358 (2001) 135–138, https://doi.org/10.1016/S0140-6736(01)05321-1.

[11] T.J. Foster, The Staphylococcus aureus "superbug", J. Clin. Invest. 114 (2004) 1693–1696, https://doi.org/10.1172/JCI23825.

[12] E. Binda, F. Marinelli, G.L. Marcone, Old and new glycopeptide antibiotics: action and resistance, Antibiotics 3 (2014) 572–594, https://doi.org/10.3390/antibiotics3040572.

[13] J. Pootoolal, J. Neu, G.D. Wright, Glycopeptide antibiotic resistance, Annu. Rev. Pharmacol. Toxicol. 42 (2002) 381–408, https://doi.org/10.1146/annurev.pharmtox.42.091601.142813.

[14] J. Hasan, R.J. Crawford, E.P. Ivanova, Antibacterial surfaces: the quest for a new generation of biomaterials, Trends Biotechnol. 31 (2013) 295–304, https://doi.org/10.1016/j.tibtech.2013.01.017.

[15] D. Campoccia, L. Montanaro, C.R. Arciola, A review of the clinical implications of anti-infective biomaterials and infection-resistant surfaces, Biomaterials 34 (2013) 8018–8029, https://doi.org/10.1016/j.biomaterials.2013.07.048.

[16] D. Campoccia, L. Montanaro, C.R. Arciola, A review of the biomaterials technologies for infection-resistant surfaces, Biomaterials 34 (2013) 8533–8554, https://doi.org/10.1016/j.biomaterials.2013.07.089.

[17] S. Chen et al., Surface hydration: principles and applications toward low-fouling/nonfouling biomaterials, Polymer 51 (2010) 5283–5293, https://doi.org/10.1016/j.polymer.2010.08.022.

[18] S. Krishnan, C.J. Weinman, C.K. Ober, Advances in polymers for anti-biofouling surfaces, J. Mater. Chem. 18 (2008) 3405–3413, https://doi.org/10.1039/B801491D.

[19] E.-R. Kenawy, S.D. Worley, R. Broughton, The chemistry and applications of antimicrobial polymers: a state-of-the-art review, Biomacromolecules 8 (2007) 1359–1384, https://doi.org/10.1021/bm061150q.

[20] M.R.E. Santos et al., Recent developments in antimicrobial polymers: a review, Materials 9 (2016) 599, https://doi.org/10.3390/ma9070599.

[21] Y. Yang et al., Antimicrobial cationic polymers: from structural design to functional control, Polym. J. 50 (2018) 33–44, https://doi.org/10.1038/pj.2017.72.

[22] M. Zasloff, Antimicrobial peptides of multicellular organisms, Nature 415 (2002) 389–395, https://doi.org/10.1038/415389a.

[23] E.M. Hetrick, M.H. Schoenfisch, Reducing implant-related infections: active release strategies, Chem. Soc. Rev. 35 (2006) 780–789, https://doi.org/10.1039/B515219B.

[24] K.P. Miller et al., Inorganic nanoparticles engineered to attack bacteria, Chem. Soc. Rev. 44 (2015) 7787–7807, https://doi.org/10.1039/C5CS00041F.

[25] Y. Liu et al., Nanotechnology-based antimicrobials and delivery systems for biofilm-infection control, Chem. Soc. Rev. 48 (2019) 428–446, https://doi.org/10.1039/C7CS00807D.

[26] D. Campoccia et al., Antibiotic-loaded biomaterials and the risks for the spread of antibiotic resistance following their prophylactic and therapeutic clinical use, Biomaterials 31 (2010) 6363–6377, https://doi.org/10.1016/j.biomaterials.2010.05.005.

[27] M.M. Harriott, M.C. Noverr, Candida albicans and Staphylococcus aureus form polymicrobial biofilms: effects on antimicrobial resistance, Antimicrob. Agents Chemother. 53 (2009) 3914–3922, https://doi.org/10.1128/AAC.00657-09.

[28] L. Eisoldt, A. Smith, T. Scheibel, Decoding the secrets of spider silk, Mater. Today 14 (2011) 80–86, https://doi.org/10.1016/S1369-7021(11)70057-8.

[29] J.A. Kluge et al., Spider silks and their applications, Trends Biotechnol. 26 (2008) 244–251, https://doi.org/10.1016/j.tibtech.2008.02.006.

[30] S. Wright, S.L. Goodacre, Evidence for antimicrobial activity associated with common house spider silk, BMC Res. Notes 5 (2012) 326, https://doi.org/10.1186/1756-0500-5-326.

[31] A. Sponner et al., Composition and hierarchical organisation of a spider silk, PLOS ONE 2 (2007) e998, https://doi.org/10.1371/journal.pone.0000998.

[32] A.R. Franco et al., Silk-based antimicrobial polymers as a new platform to design drug-free materials to impede microbial infection, Macromol. Biosci. 18 (2018) 1800262, https://doi.org/10.1002/mabi.201800262.

[33] L. Nilebäck et al., Self-assembly of recombinant silk as a strategy for chemical-free formation of bioactive coatings: a real-time study, Biomacromolecules 18 (2017) 846–854, https://doi.org/10.1021/acs.biomac.6b01721.

[34] R.H. Zha et al., Universal nanothin silk coatings via controlled spidroin self-assembly, Biomater. Sci. 7 (2019) 683–695, https://doi.org/10.1039/C8BM01186A.

[35] S. Zhang et al., Nitrogen inaccessibility protects spider silk from bacterial growth, J. Exp. Biol. 222 (2019) jeb214981, https://doi.org/10.1242/jeb.214981.

[36] D. Huemmerich et al., Primary structure elements of spider dragline silks and their contribution to protein solubility, Biochemistry 43 (2004) 13604–13612, https://doi.org/10.1021/bi048983q.

[37] C. Vendrely, T. Scheibel, Biotechnological production of spider-silk proteins enables new applications, Macromol. Biosci. 7 (2007) 401–409, https://doi.org/10.1002/mabi.200600255.

[38] A. Leal-Egaña, T. Scheibel, Silk-based materials for biomedical applications, Biotechnol. Appl. Biochem. 55 (2010) 155–167, https://doi.org/10.1042/BA20090229.

[39] S. Müller-Herrmann, T. Scheibel, Enzymatic degradation of films, particles, and nonwoven meshes made of a recombinant spider silk protein, ACS Biomater. Sci. Eng. 1 (2015) 247–259, https://doi.org/10.1021/ab500147u.

[40] P.H. Zeplin et al., Spider silk coatings as a bioshield to reduce periprosthetic fibrous capsule formation, Adv. Funct. Mater. 24 (2014) 2658–2666, https://doi.org/10.1002/adfm.201302813.

[41] C.B. Borkner et al., Surface modification of polymeric biomaterials using recombinant spider silk proteins, ACS Biomater. Sci. Eng. 3 (5) (2017) 767–775, https://doi.org/10.1021/acsbiomaterials.6b00306.

[42] F. Bauer, S. Wohlrab, T. Scheibel, Controllable cell adhesion, growth and orientation on layered silk protein films, Biomater. Sci. 1 (2013) 1244–1249, https://doi.org/10.1039/C3BM60114E.

[43] A. Leal-Egana et al., Interactions of fibroblasts with different morphologies made of an engineered spider silk protein, Adv. Eng. Mater. 14 (2012) B67–B75, https://doi.org/10.1002/adem.201180072.

[44] S. Wohlrab et al., Cell adhesion and proliferation on RGD-modified recombinant spider silk proteins, Biomaterials 33 (2012) 6650–6659, https://doi.org/10.1016/j.biomaterials.2012.05.069.

[45] K. Schacht et al., Biofabrication of cell-loaded 3D spider silk constructs, Angew. Chem. Int. Ed. 54 (2015) 2816–2820, https://doi.org/10.1002/anie.201409846.
[46] K. Schacht, U. Slotta, M. Suhre, Prevention of biofilm formation with vegan silk polypeptides, Sofw J 143 (2017) 04.
[47] M.V. Graham, N.C. Cady, Nano and microscale topographies for the prevention of bacterial surface fouling, Coatings 4 (2014) 37–59, https://doi.org/10.3390/coatings4010037.
[48] X. Khoo, M.W. Grinstaff, Novel infection-resistant surface coatings: a bioengineering approach, MRS Bulletin 36 (2011) 357–366, https://doi.org/10.1557/mrs.2011.66.
[49] A. Tripathy et al., Natural and bioinspired nanostructured bactericidal surfaces, Adv. Colloid Interface Sci. 248 (2017) 85–104, https://doi.org/10.1016/j.cis.2017.07.030.
[50] S. Erramilli, J. Genzer, Influence of surface topography attributes on settlement and adhesion of natural and synthetic species, Soft Matter 15 (2019) 4045–4067, https://doi.org/10.1039/C9SM00527G.
[51] Y. Cheng, G. Feng, C.I. Moraru, Micro- and nanotopography sensitive bacterial attachment mechanisms: a review, Front. Microbiol. 10 (2019) 191, https://doi.org/10.3389/fmicb.2019.00191.
[52] M. Humenik et al., Ion and seed dependent fibril assembly of a spidroin core domain, J. Struct. Biol. 191 (2015) 130–138, https://doi.org/10.1016/j.jsb.2015.06.021.
[53] U. Slotta et al., Structural analysis of spider silk films, Supramol. Chem. 18 (2006) 465–471, https://doi.org/10.1080/10610270600832042.
[54] E. Metwalli et al., Structural changes of thin films from recombinant spider silk proteins upon post-treatment, Appl. Phys. A 89 (2007) 655–661, https://doi.org/10.1007/s00339-007-4265-5.
[55] K. Spiess, A. Lammel, T. Scheibel, Recombinant spider silk proteins for applications in biomaterials, Macromol. Biosci. 10 (2010) 998–1007, https://doi.org/10.1002/mabi.201000071.
[56] S. Wohlrab, K. Spieß, T. Scheibel, Varying surface hydrophobicities of coatings made of recombinant spider silk proteins, J. Mater. Chem. 22 (2012) 22050–22054, https://doi.org/10.1039/C2JM35075K.
[57] S. Kumari et al., Recombinant spider silk hydrogels for sustained release of biologicals, ACS Biomater. Sci. Eng. 4 (2018) 1750–1759, https://doi.org/10.1021/acsbiomaterials.8b00382.
[58] E. DeSimone et al., Recombinant spider silk-based bioinks, Biofabrication 9 (2017) 044104, https://doi.org/10.1088/1758-5090/aa90db.
[59] C. Thamm, E. DeSimone, T. Scheibel, Characterization of hydrogels made of a novel spider silk protein eMaSp1s and evaluation for 3D printing, Macromol. Biosci. 17 (2017) 1700141, https://doi.org/10.1002/mabi.201700141.
[60] B. Dhandayuthapani et al., Polymeric scaffolds in tissue engineering application: a review, Int. J. Polym. Sci. 2011 (2011) 290602, https://doi.org/10.1155/2011/290602.
[61] J. Jang, H.-G. Yi, D.-W. Cho, 3D printed tissue models: present and future, ACS Biomater. Sci. Eng. 2 (2016) 1722–1731, https://doi.org/10.1021/acsbiomaterials.6b00129.
[62] S. Kumari, et al., Data for microbe resistant engineered recombinant spider silk protein based 2D and 3D materials. Data in Brief, submitted for publication (2020).
[63] N. Thewes et al., A detailed guideline for the fabrication of single bacterial probes used for atomic force spectroscopy, Eur. Phys. J. E 38 (2015) 140, https://doi.org/10.1140/epje/i2015-15140-2.
[64] C. Spengler et al., Strength of bacterial adhesion on nanostructured surfaces quantified by substrate morphometry, Nanoscale 11 (2019) 19713–19722, https://doi.org/10.1039/C9NR04375F.
[65] A. Beaussart et al., Single-cell force spectroscopy of probiotic bacteria, Biophys J. 104 (2013) 1886–1892, https://doi.org/10.1016/j.bpj.2013.03.046.
[66] G. Zeng, T. Müller, R.L. Meyer, Single-cell force spectroscopy of bacteria enabled by naturally derived proteins, Langmuir 30 (2014) 4019–4025, https://doi.org/10.1021/la404673q.
[67] T. Jungst et al., Strategies and molecular design criteria for 3D printable hydrogels, Chem. Rev. 116 (2016) 1496–1539, https://doi.org/10.1021/acs.chemrev.5b00303.
[68] D.N. Rockwood et al., Materials fabrication from Bombyx mori silk fibroin, Nat. Protoc. 6 (2011) 1612–1631, https://doi.org/10.1038/nprot.2011.379.
[69] H. Shirahama et al., Precise tuning of facile one-pot gelatin methacryloyl (GelMA) synthesis, Sci. Rep. 6 (2016) 31036, https://doi.org/10.1038/srep31036.
[70] B.J. Klotz et al., Gelatin-methacryloyl hydrogels: towards biofabrication-based tissue repair, Trend Biotechnol. 34 (2016) 394–407, https://doi.org/10.1016/j.tibtech.2016.01.002.
[71] C.B. Borkner et al., Ultrathin spider silk films: insights into spider silk assembly on surfaces, ACS Appl. Polym. Mater. 1 (2019) 3366–3374, https://doi.org/10.1021/acsapm.9b00792.
[72] A.M. Anton et al., Foundation of the outstanding toughness in biomimetic and natural spider silk, Biomacromolecules 18 (2017) 3954–3962, https://doi.org/10.1021/acs.biomac.7b00990.
[73] C. Guo et al., Structural comparison of various silkworm silks: an insight into the structure-property relationship, Biomacromolecules 19 (2018) 906–917, https://doi.org/10.1021/acs.biomac.7b01687.